

# **Nonlinear Finite Element Analysis of Insulated FRP Strengthened Reinforced Concrete Columns Subjected to Fire**

M. Hisham\*, O. El-Mahdy\*\* and G. Hamdy\*\*\*

\*Teaching Assistant, \*\*Professor of Structural Analysis, \*\*\*Associate Professor,  
Civil Engineering Department, Faculty of Engineering at Shoubra, Benha University, Egypt  
108 Shoubra Street, Shoubra, Cairo 11241, Egypt

## **Abstract**

Recently, Fiber Reinforced Polymers (FRP) have been successfully used for retrofitting or strengthening of existing concrete structural members due to its superior properties such as high strength, corrosion resistance and ease of application. However, its behavior under elevated temperature likely to occur in case of fire is a problem that presents a threat to the strengthened member. This paper presents numerical investigation of reinforced concrete (RC) columns strengthened with FRP and insulated by a thermal resisting coating under service load and fire conditions. The finite element numerical modeling and nonlinear analysis are made using the general purpose software ANSYS 12.1. Numerical modeling is made for FRP-strengthened and insulated RC columns that have been experimentally tested under standard fire tests in the published literature. The obtained numerical results are in good agreement with the experimental ones regarding the temperature distribution and axial deformations. Thus, the presented modeling gives an economic tool to investigate the performance of loaded FRP strengthened columns under high temperatures. Furthermore, the model can be used to design thermal protection layers for FRP strengthened RC columns to satisfy fire resistance requirements specified in building codes and standards.

**Keywords:** Nonlinear analysis, finite elements, modeling, RC columns, FRP, axial strengthening, confinement, fire, thermal insulation.

## **1. Introduction**

Fiber Reinforced Polymers (FRP) have showed outstanding potential as a material for repair, retrofit or strengthening existing reinforced concrete (RC) members that have been destroyed via factors such as chemical corrosion and increased load conditions. The increasing use of FRP in strengthening applications is due to their high strength, durability and excellent corrosion resistance. However, their poor performance under fire presents a threat to the

strengthened member since they are usually applied on the outer surface of the structural elements and the strengthening may be totally lost in case of fire [add reference here]. Research work is required to investigate the behavior of FRP strengthened isolated structural concrete members under fire conditions. Some experimental researches have been conducted where FRP strengthened columns are tested in standard fire tests. However, few numerical studies addressed the behavior of these elements; especially FRP strengthened and isolated RC columns, under realistic fire loads. Hence, more investigation work is needed to model numerically the behavior of FRP-strengthened RC columns under elevated temperatures in order to enable designers to accurately predict the fire endurance and residual strength and provide efficient design of thermal insulation layers for these structures.

The present paper aims to investigate numerically the performance of RC columns confined by FRP and thermally protected with insulation material under service load and standard fire test loading. To achieve this goal, numerical modeling by finite elements is made that represents the column geometry and considers the variation in thermal and mechanical properties of the different constituent materials with elevated temperature. Numerical modeling and nonlinear analysis are made using the software ANSYS v.12.1.0 [2]. A numerical study is conducted for FRP strengthened and insulated columns that have been previously tested experimentally under standard fire test. The numerical modeling results are presented and compared to published experimental and numerical results so as to verify the efficiency of the adopted numerical procedure. Finally, the conclusions of the study are given.

## **2. Literature Review**

One of the most useable applications of FRPs is strengthening of RC columns. This can be done into two different ways, first by applying FRP sheets to the longitudinal direction of the column in order to provide additional flexural capacity, or by applying FRP sheets in circumferential direction in order to provide additional axial confining reinforcement which increase both compressive strength and ductility of RC columns. Youssef et al. [3] developed a semi-empirical model for FRP confinement based on large scale experimental program that predict confined strength of RC column ( $f'_{cu}$ ) and axial confined strain ( $\epsilon_{cu}$ ).

Experimental studies were carried out to investigate the performance of FRP strengthened RC columns under fire condition by several researchers [4, 5]. In order to provide protection of FRP from fire exposure, a coating layer material of thermal resisting properties, typically gypsum products, may be placed around the columns. In a fire test program conducted by Bisby [6], two CFRP-strengthened RC columns protected with vermiculite-gypsum (VG) cementitious layers with different thickness were subjected to service loads and exposed to standard fire load of ASTM E119 [7]. The study includes experimental and numerical results for both thermal and structural aspects. Using an insulation layer with proper thickness managed to increase the fire time endurance to above five hours of fire exposure [6].

Few previous studies in the published literature addressed numerical modeling to predict the performance of FRP-strengthened RC members subjected to fire with multiple types of protection systems [8, 9]. Therefore, more investigation work is needed to model efficiently the behavior of FRP-strengthened RC columns under elevated temperatures, in order to accurately predict the fire endurance and residual strength.

### 3. Variation of Materials Properties with Elevated Temperature

This section describes variation of the physical and mechanical properties of constituent materials with elevated temperature, as presented in the literature.

#### 3.1 Density

The steel reinforcement density is considered by Eurocode 3 (2005) [10] to remain constant under elevated temperature. The variation of density of concrete with elevated temperature is given by Eq. (1) [11] as follows:

$$\rho(T) = \rho(20^{\circ}C) \quad \text{For } 20^{\circ}C \leq T \leq 115^{\circ}C \quad (1. a)$$

$$\rho(T) = \rho(20^{\circ}C) \left( 1 - \frac{0.02(T - 115)}{85} \right) \quad \text{For } 115^{\circ}C < T \leq 200^{\circ}C \quad (1. b)$$

$$\rho(T) = \rho(20^{\circ}C) \left( 0.98 - \frac{0.03(T - 200)}{200} \right) \quad \text{For } 200^{\circ}C < T \leq 400^{\circ}C \quad (1. c)$$

$$\rho(T) = \rho(20^{\circ}C) \left( 0.95 - \frac{0.07(T - 400)}{800} \right) \quad \text{For } 400^{\circ}C < T \leq 1200^{\circ}C \quad (1. d)$$

### 3.2 Thermal conductivity

The variation of thermal conductivity of concrete with temperature is given by Eq. (2). Equation (3) gives the variation in thermal conductivity of steel reinforcement with temperature.

$$K(T) = 2 - 0.2451 \left( \frac{T}{100} \right) + 0.0107 \left( \frac{T}{100} \right)^2 \quad \text{For } 20^\circ\text{C} \leq T \leq 1200^\circ\text{C} \quad (2)$$

$$K(T) = 54 - 3.33 \times 10^{-2} T \quad \text{in } \left( \frac{W}{m} \cdot K \right) \quad \text{For } 20^\circ\text{C} \leq T \leq 800^\circ\text{C} \quad (3. a)$$

$$K(T) = 27.30 \quad \text{in } \left( \frac{W}{m} \cdot K \right) \quad \text{For } 800^\circ\text{C} < T \leq 800^\circ\text{C} \quad (3. b)$$

### 3.3 Specific heat

The variation of specific heat of concrete with temperature is given by Eq (4). The peak specific heat of concrete depends mainly on the moisture content and occurs between 100°C and 115°C with linear decrease between 115°C and 200°C. For zero moisture content the peak specific heat is 900 J/kg K, while for moisture content 1.5 % and 3% of concrete weight the peak specific heat is 1470 J/kg K and 2020 J/kg K, respectively.

$$C(T) = 900 \quad \text{in } \left( \frac{J}{Kg} \cdot K \right) \quad \text{For } 20^\circ\text{C} \leq T \leq 100^\circ\text{C} \quad (4. a)$$

$$C(T) = 900 + (T - 100) \quad \text{in } \left( \frac{J}{Kg} \cdot K \right) \quad \text{For } 100^\circ\text{C} < T \leq 200^\circ\text{C} \quad (4. b)$$

$$C(T) = 1000 + \frac{(T - 200)}{2} \quad \text{in } \left( \frac{J}{Kg} \cdot K \right) \quad \text{For } 200^\circ\text{C} < T \leq 400^\circ\text{C} \quad (4. c)$$

$$C(T) = 1100 \quad \text{in } \left( \frac{J}{Kg} \cdot K \right) \quad \text{For } 400^\circ\text{C} < T \leq 1200^\circ\text{C} \quad (4. d)$$

Equation (5) shows the change in specific heat for steel reinforcement with temperature as given by Eurocode2 (2005), for temperature range between 20°C to 1200°C.

For  $20^\circ\text{C} \leq T \leq 600^\circ\text{C}$

$$C(T) = 425 + 7.73 \times 10^{-1} T - 1.69 \times 10^{-3} T^2 + 2.22 \times 10^{-6} T^3 \quad \text{in } \left( \frac{J}{Kg} \cdot K \right) \quad (5. a)$$

$$C(T) = 666 + \left( \frac{13002}{738 - T} \right) \text{in } \left( \frac{J}{Kg} \cdot K \right) \quad \text{For } 600^\circ\text{C} < T \leq 735^\circ\text{C} \quad (5. b)$$

$$C(T) = 545 + \left( \frac{17820}{T - 731} \right) \text{in } \left( \frac{J}{Kg} \cdot K \right) \quad \text{For } 735^\circ\text{C} \leq T < 900^\circ\text{C} \quad (5. c)$$

$$C(T) = 650 \quad \text{in } \left( \frac{J}{Kg} \cdot K \right) \quad \text{For } 900^\circ\text{C} \leq T \leq 1200^\circ\text{C} \quad (5. d)$$

Anderberg and Thelandersson [12] proposed a model for predicting transient creep which is linearly proportional to the applied stress and thermal expansion strain of aggregate according to Eq. (6).

$$\varepsilon_{tr} = K \left( \frac{\sigma}{\sigma_u} \right) \varepsilon_{exp} \quad (6)$$

where  $K$  is a factor that depends on aggregate type and is equal to 1.8 for siliceous aggregate and 2.35 for carbonate aggregate,  $\sigma$  is the applied stress,  $\sigma_u$  is the compressive strength and  $\varepsilon_{exp}$  is thermal expansion of aggregate.

### 3.4 Stress-strain relation

The stress strain-curve for confined concrete under different temperatures are given by Youssef et al. [3] as shown in Fig. (1). On the other hand, the variation of the mechanical and the thermal properties of FRP and the materials used for thermal insulation is addressed in researches and not quite established. In this study, the thermal and mechanical properties of CFRP and VG insulation and their variation with temperature are based on the findings of other researchers such as Bisby [6], Bai et al. [13], Griffiths et al. [14], Cramer et al. [15] and Park et al. [16].

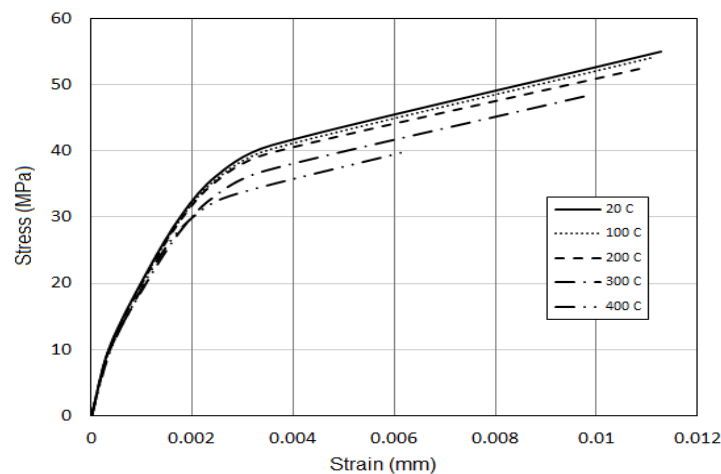


Figure. (1) Variation of Stress-Strain Relations for Confined Concrete with Temperature [3]

## 4. Finite Element Formulation and Nonlinear Solution Procedure

Numerical modeling is made by finite elements for FRP-strengthened and insulated RC columns under vertical loading and subjected to elevated temperature. The finite element modeling and nonlinear analysis is performed using ANSYS 12.1 software. The element types used to represent the different materials are given in Table 1.

The numerical model takes into account the variation in thermal and mechanical properties of the concrete, steel rebar, FRP and insulation material. The values adopted in the present study for the mechanical and thermal properties of the constituent materials at room temperature are listed in Table 2.

Table 1 Element Types Used for Thermal and Structural Analyses

Material	Thermal analysis	Structural analysis
Concrete	SOLID70	SOLID65
Steel bars	LINK33	LINK8
CFRP layer	SHELL 57	SHELL 41
VG insulation	SOLID70	SOLID 45

Table 2 Mechanical and Thermal Material Properties at Room Temperature [17, 18]

Material	$E_o$ MPa	$K_o$	$C_o$	$\mu$	$\alpha$	$\rho_o$
Concrete	29725	$2.7 \times 10^{-3}$	722.8	0.2	$6.08 \times 10^{-6}$	2400
Steel bars	210000	$5.2 \times 10^{-2}$	452.2	0.3	$6.00 \times 10^{-6}$	7860
CFRP	95200	$1.3 \times 10^{-3}$	1310	0.28	$-0.90 \times 10^{-5}$	1600
VG	2100	$2.5 \times 10^{-4}$	1654	0.3	$1.70 \times 10^{-5}$	269

Concrete is modeled using the standard nonlinear constitutive concrete material model implemented within ANSYS. When a crack occurs, elastic modulus of the concrete element is set to zero in the direction parallel to the principal tensile stress direction. Crushing results when all principal stresses are compressive and are outside the failure surface; then the elastic modulus is set to zero in all directions and the element local stiffness becomes zero causing large displacement and divergence in the solution. The time temperature relation of the ASTM E119 standard fire test is shown in Fig. (2) and is given in eq. (7).

$$Tg = 20 + 750 (1 - e^{-0.49\sqrt{t}}) + 22\sqrt{t} \quad (7)$$

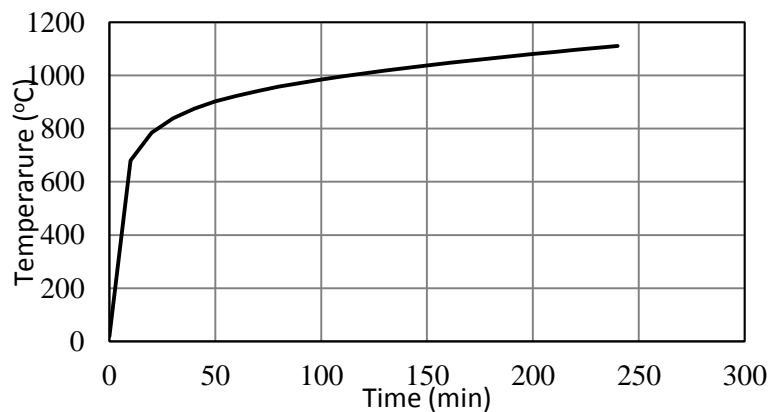


Figure. (2) Applied Temperature Conforming to Standard Fire Test Curve of ASTM E119 [7]

## 5. Numerical Study

### 5.1 Description

Finite element modeling is made for FRP-strengthened RC columns that were subjected to fire test by Bisby [6]. The columns had length of 3810 mm and circular cross section of 400 mm diameter. The columns were confined by single layer of CFRP layer with thickness of 0.76 mm. The strengthening system was Tyfo SCH System with Tyfo S Epoxy. The column was thermally protected using Tyfo® VG insulation. The thickness of VG protection layer for first and second column was 32, 57 mm respectively as shown in Figs. (3, 4).

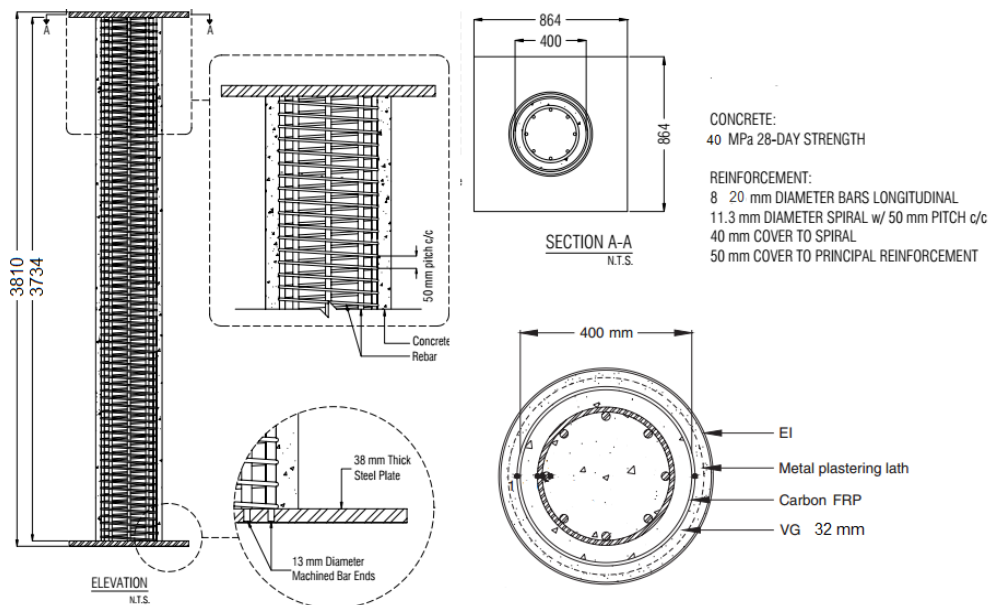


Figure. (3) Column (1): Column Dimensions and Reinforcement Details [6]

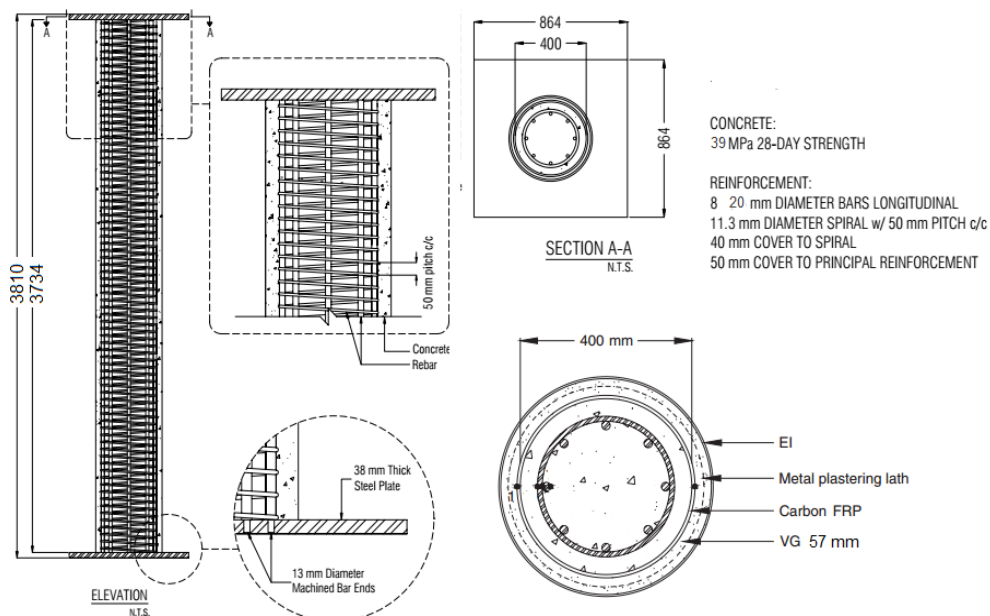


Figure. (4) Column (2): Column Dimensions and Reinforcement Details [6]

## 5.2 Finite element modeling and material properties

The element types used for thermal and structural finite element analysis are given in Table 1. As the section of the columns is symmetric about x and z axes therefore, only quarter of the section was modeled in ANSYS as shown in Figs. (5, 6).

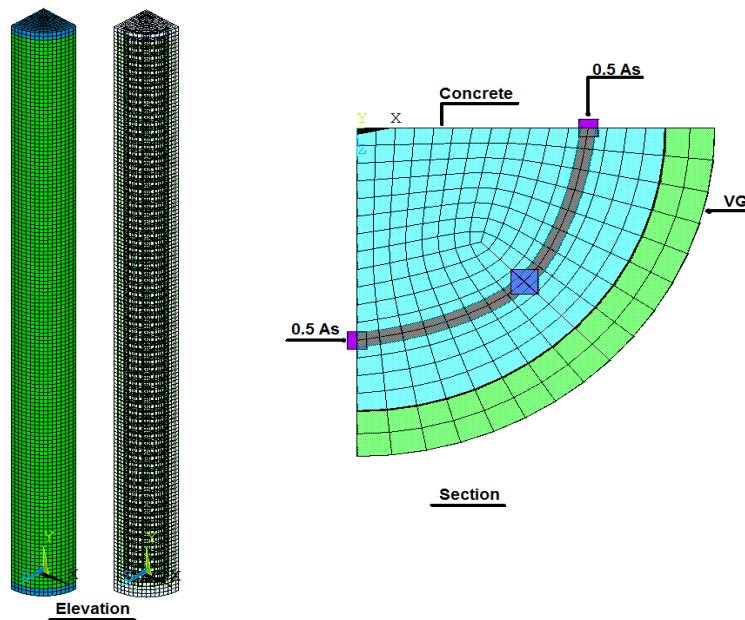


Figure. (5) Column (1): 3-D Finite Element Model

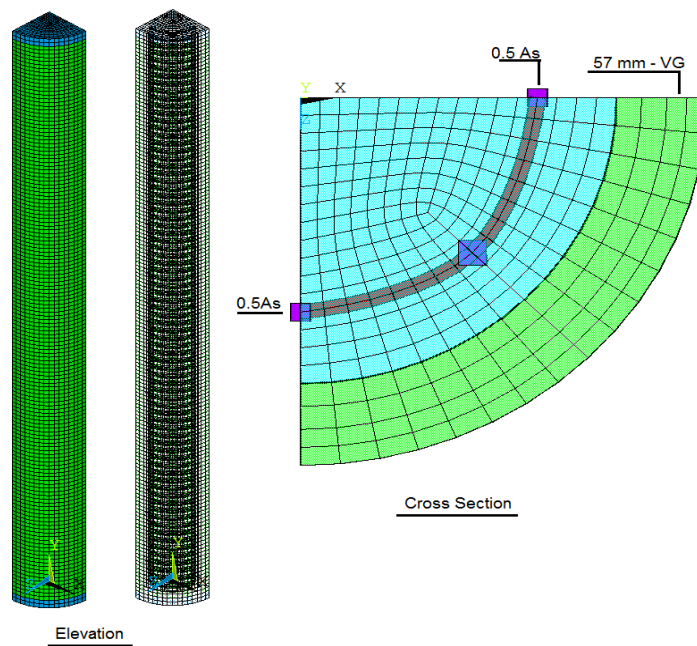


Figure. (6) Column (2): 3-D Finite Element Model



The average concrete compressive strengths for column (1) and column (2) were 40 MPa and 39 MPa, respectively. The RC columns were cast using carbonate aggregate. Moisture content equal to 7 % of concrete weight is adopted. Yield strength for both longitudinal and transverse reinforcements was 400 MPa. CFRP has 1.2% strain at rupture and ultimate tensile strength is 1351 MPa. The values for the mechanical and thermal properties of the constituent materials at room temperature are as given in Table 2.

### **5.3 Nonlinear solution parameters, loading and boundary conditions**

The analysis is carried out as two consecutive load cases. First, the transient thermal analysis load case, standard temperature-time conditions described by ASTM E119 and shown in Fig. (2) are applied as nodal temperature-versus-time to outer surface of the column. Second, the structural analysis consists of two cumulative load steps, in the first load step the vertical load increasing gradually until service load 2515 kN and temperature is constant at 20°C for one hour, then second load starts with constant vertical load of 2515 kN and the temperature of this load steps vary according to thermal analysis that has been conducted in thermal model for five hours. If the column did not fail after passing specified analysis time, the model increases service load gradually until failure.

## **6. Numerical Results and Discussion**

In order to validate the accuracy of the developed model, the obtained numerical results are compared to the experimental and numerical results. The thermal analyses results are estimated by checking the temperatures at key locations with temperature gradients between the key locations of the column model. The nodal temperature distribution within the columns different time of fire exposure are shown in Figs. (7,8).

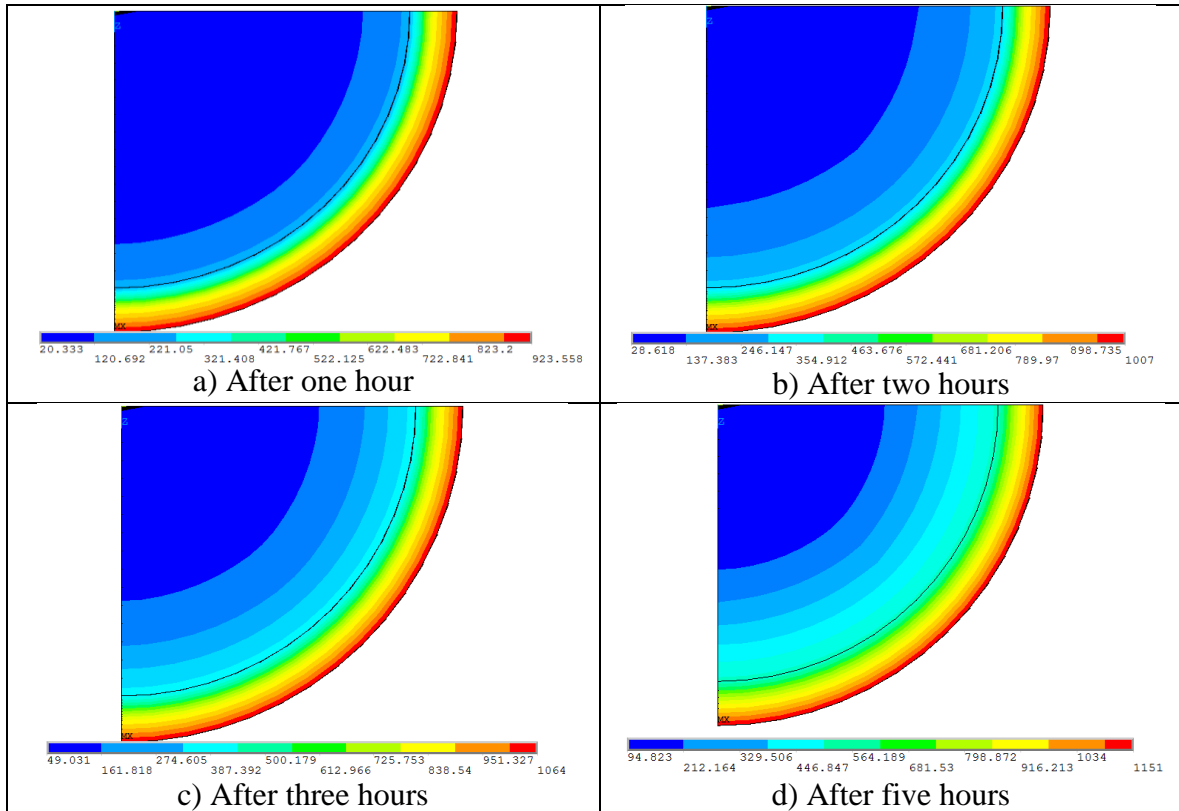


Figure. (1) Column (1): Thermal Distribution Predicted Within the Column Cross-Section

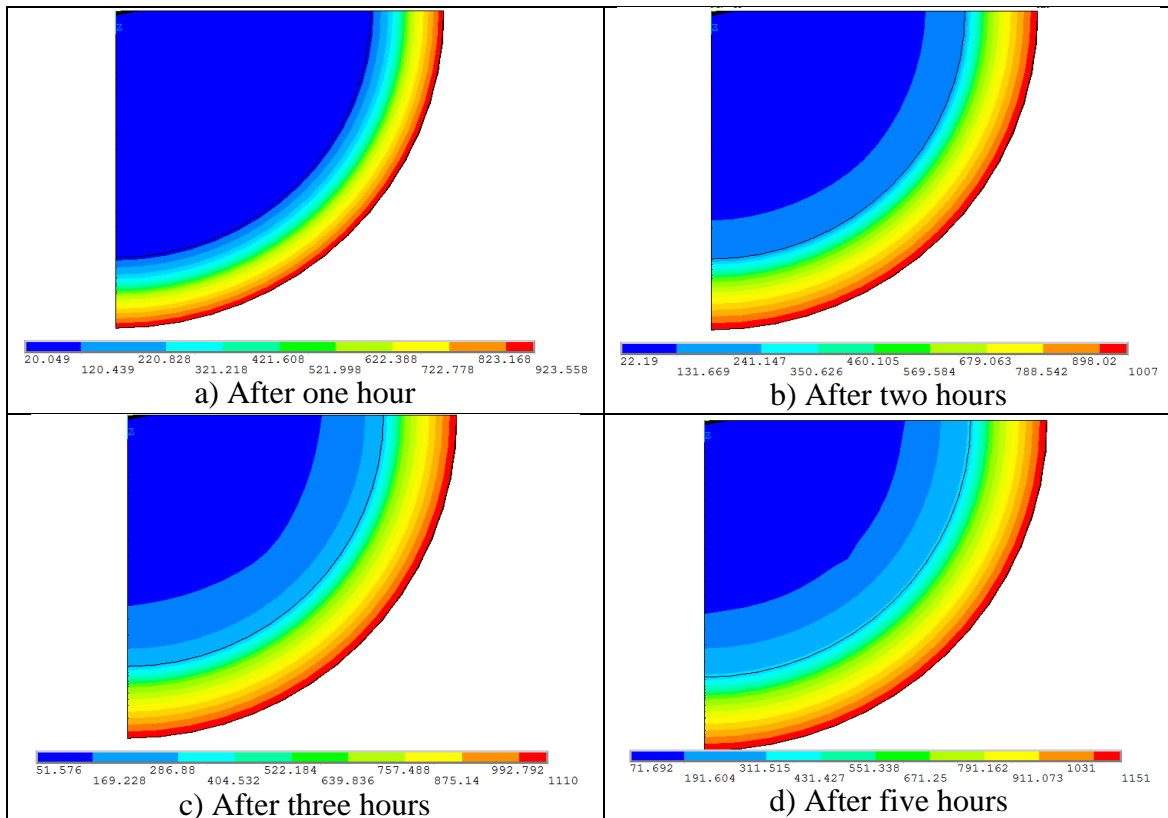


Figure. (2) Column (2): Thermal Distribution Predicted Within the Column Cross-Section

The variation with time of the numerically calculated temperatures in concrete, CFRP, and RFT at the same points that were measured in the experiment work of Bisby (2003) are plotted in Figs. (9, 10).

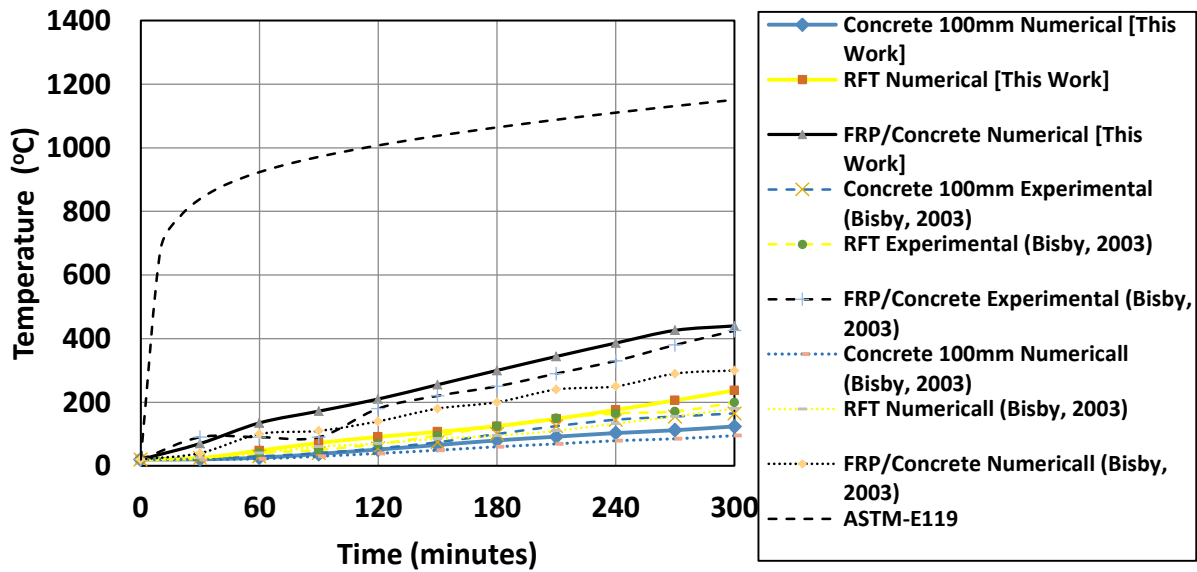


Figure. (3) Column (1): Thermal Results for Numerical Models and Experimental Results

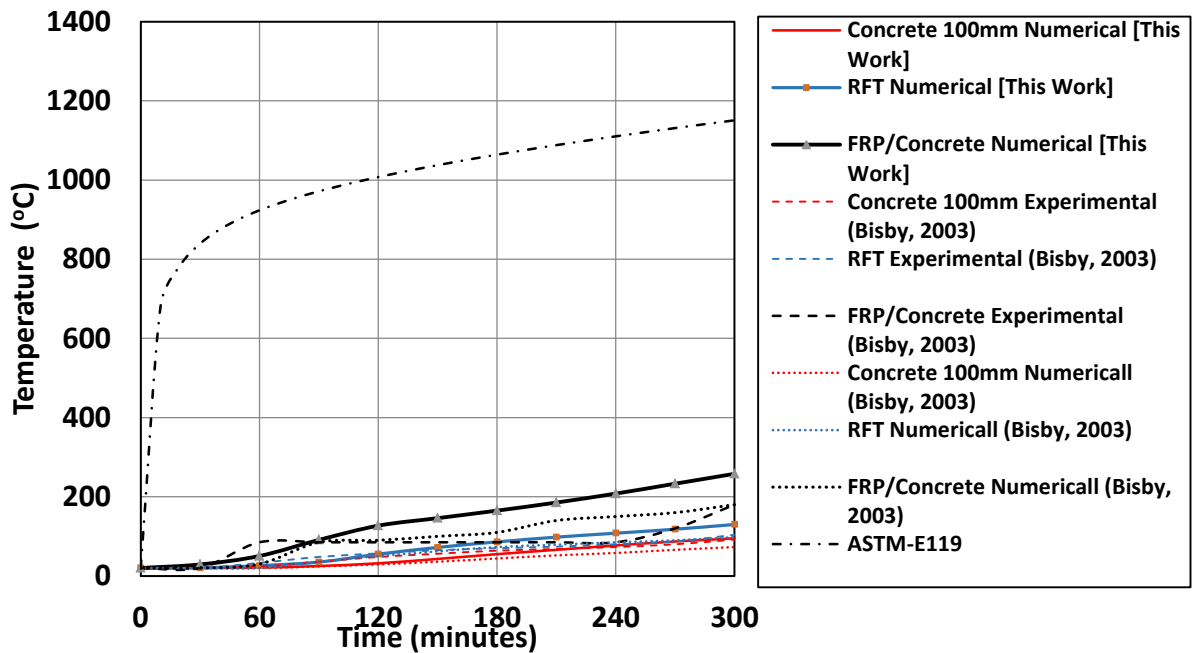


Figure. (4) Column (2): Thermal Results for Numerical Models and Experimental Results

Figures (11,12) show the numerically predicted and the experimentally measured axial deformation under the applied service load and fire exposure for specific period of time for both columns. It can be concluded that, the predicted results are in good agreement with experimental ones. Furthermore, the present numerical results are better than those obtained

by Bisby's model due to consideration of the transient creep effect in finite element model. The failure load value of the experimental and the present model are 4473 and 5018 KN for column (1). As for column (2) failure load value of the experimental and the present model are 4680 and 5393 KN, respectively. It should be mentioned that, structural RC members such as column typically require fire endurance ratings greater than four hours and the fire endurance time for both analytical and experimental work was more than five hours.

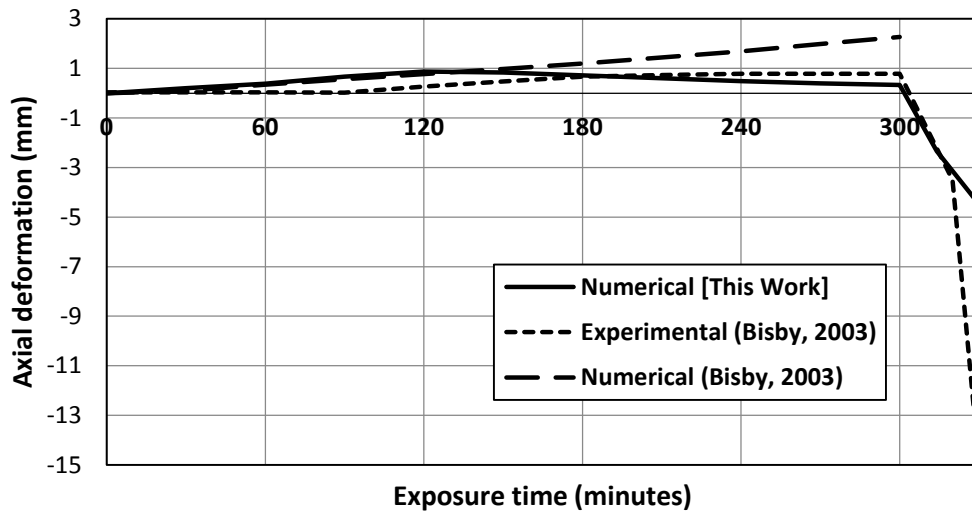


Figure. (5) Column (1): Axial Deformations Response

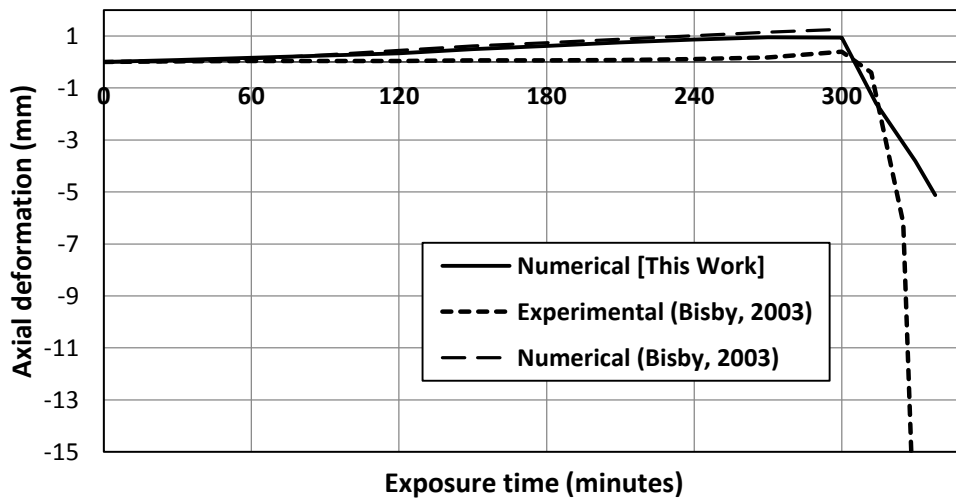


Figure. (6) Column (2): Axial Deformations Response

## 7. Conclusions

The paper presents numerical modeling procedure by finite elements that simulates the behavior of thermally insulated RC column confinement with CFRP laminate when exposed to standard fire test. Numerical modeling and nonlinear analysis are performed using ANSYS 12.1. The proposed procedure is verified by comparing the numerical results with

experimental results in the published literature. Based on the obtained numerical results, the following conclusions can be drawn.

1. The numerical results of the proposed model are in good agreement with experimental results for both thermal and structural aspects.
2. The proposed model gives more accurate axial deformation response compared with published numerical results due to consideration of transient creep strain.
3. The proposed model can accurately predict thermal and structural response for different configurations regarding material properties or insulation thickness and type.
4. The axial deformation response for column under fire tend to expand in early stage of fire exposure followed by contraction due to degradation in stiffness and presence of transient creep strain which acts against expansion strain of burned column.
5. The proposed model provides an economic tool for check and design fire insulation layers for FRP strengthened RC columns.

## References

1. ....
2. ANSYS–Release Version 12.1.0, “A Finite Element Computer Software and User Manual for Nonlinear Structural Analysis”, ANSYS Inc. Canonsburg, PA., (2009).
3. Youssef, M. N., Feng, M. Q. and Masallam, A. S., “Stress-Strain Model for Concrete Confined by FRP Composites”, *Composites Part B*, V. 38, pp. 614-628, (2007).
4. Chowdhury, E.U, Bisby, L.A. and Green, M.F., "Investigation of Insulated FRP-Wrapped Reinforced Concrete Columns in Fire", *Fire Safety Journal*, 42 (2007), pp. 452–460.
5. Cree, C., Chowdhury, E.U., Bisby, L.A., Green, M.F., and Benichou, N., “Performance in Fire of FRP-Strengthened and Insulated Reinforced Concrete Columns”, *Fire Safety Journal*, 54 (2012), pp. 86–95.
6. Bisby, L. A., “Fire Behavior of FRP Reinforced or Confined Concrete.”, PhD thesis, Dept. of Civil Engineering Queen’s Univ., Kingston, Ont., Canada, (2003).
7. ASTM, "Standard Test Methods for Fire Tests of Building Construction and Materials", ASTM Standard E119, American Society for Testing of Materials, West Conshohocken, PA, (2002).

8. Bikhiet, M.M., El-Shafey, N.F. and El-Hashimy, H.M., "Behavior of Reinforced Concrete Short Columns Exposed to Fire", Alexandria Engineering Journal, 53, 643–653, (2014).
9. Bisby, L.A., Green, M.F. and Kodur, V.K.R., "Modeling the Behavior of Fiber Reinforced Polymer-Confined Concrete Columns Exposed to Fire", 10.1061/(ASCE)1090-0268(2005) 9:1(15).
10. Eurocode 3, "Design of Steel Structures, ENV EC3 Part 1.2.", Eurocode, (2005).
11. Eurocode2, "Design of Concrete Structures, ENV EC2 Part 1.2", Eurocode, (2004).
12. Anderberg, Y. and Thelandersson, S., "Stress and Deformation Characteristics of Concrete at High Temperature: 2. Experimental Investigation and Material Behavior Model", Bull. No. 46, Lund, (1976).
13. Bai, Y., Keller, T., and Vallée, T., "Modeling of Stiffness of FRP Composites under Elevated and High temperatures", Compos. Sc. Techn., 68 (15-16) (2008) 3309–3106.
14. Griffis, C., Masmura, R. and Chang, C., "Thermal Response of Graphite Epoxy Composite Subjected to Rapid Heating", Environmental Effects on Composite Materials, Vol. 2, pp. 245- 260, (1984).
15. Cramer, S.M., Friday, O.M., White, R.H., and Sriprutkiat, G., "Mechanical Properties of Gypsum Board at Elevated Temperatures", Fire and Materials (2003) 33–42.
16. Park, S. H., Manzello, S., L., Bentz, D., P., and Mizukami, T., "Determining Thermal Properties of Gypsum Board at Elevated Temperatures", Fire and Materials, (2009), pp. 237-250.
17. Bisby et al (2006) ???
18. Hawileh, R., A., Naser, M., Zaidan, W., and Rasheed, H. A., "Modeling of Insulated CFRP Strengthened Reinforced Concrete T-beam Exposed to Fire", Engineering Structures, 31( 12) (2009), pp. 3072–3079.
19. ECP Committee 208, ECP 208-05, "Egyptian Code of Practice for the Use of Fiber Reinforced Polymer in the Construction Field", ECP Committee 208, Ministry of Housing and Urban Communities, Egypt (2005).